Hindawi
Geofluids
Volume 2022, Article ID 7439860, 17 pages
https://doi.org/10.1155/2022/7439860

*Research Article*

# Study of the Characteristics Mechanical Damage and Constitutive Model of Crushed-Rocks from High-Grade Highway in Permafrost Region

**Qinshuai Zhang**,[1] **Qingzhi Wang**,[1,2] **Jianhong Fang**,[2] **Xiangqing Zhao**,[3] **Jizhen Li**,[1] **and Shuan Li**[1]

[1]*Qinghai University, Xining, Qinghai 810016, China*
[2]*Qinghai Research and Observation Base, Key Laboratory of Highway Construction & Maintenance Technology in Permafrost Region, Ministry of Transport, Xining, Qinghai 810016, China*
[3]*Northwest Research Institute co., Ltd of C.R.E.C, Lanzhou, Gansu 730000, China*

Correspondence should be addressed to Qingzhi Wang; wangqingzhi87@qhu.edu.cn

Received 3 February 2022; Revised 23 March 2022; Accepted 13 April 2022; Published 28 April 2022

Academic Editor: Basim Abu-Jdayil



Three types of rocks are selected to conduct uniaxial compression and microscope experimental to study the influences of freeze-thaw cycles on crushed-rocks from Gonghe-Yushu high-graded highway, which is the first high-grade highway built in permafrost regions in China. Using the hypothesis of Lemaitre's strain equivalence principle and a theoretical model of crushed-rock deterioration after freeze-thaw cycles was established and verified by the experimental data. The experimental results showed that with an increase of the number of freeze-thaw cycles, the microcracks of saturated red sandstone increased, and this phenomenon is not obvious on other rocks. Moreover, different degrees of spalling and cracks appeared, with common physical parameters gradually decreasing. The uniaxial compressive strength of rock decreases exponentially with the increase of the number of freeze-thaw cycles. The mechanism of the influence of freeze-thaw cycles on the fine structure of the three different crushed-rocks were then analyzed using SEM scanning. Freeze-thaw cycles weaken the connection between rock mineral particles and increase the surface micropores. The damage model of freeze-thaw and load can well describe the damage law of crushed-rocks.

## 1. Introduction

The permafrost area in China is approximately 2,150,000 $Km^2$, accounting for 22% of its national territory [1]. On the eastern edge of the Qinghai-Tibet Plateau, there is a high-grade highway, from Gonghe to Yushu (Gongyu) high-grade highway. It is the first high-grade highway built in the plateau permafrost area in China, as shown in Figure 1[2].

Most of the high-grade highway is above 4100 m above sea level, which is used 55.9 km of crushed-rocks embankment. The high-grade highway itself is comprised of crushed-rocks embankment, and air convection embankment [3–6]. However, the temperature difference between day and night experienced along the embankment and slope along with seasonal climate change caused by freeze-thaw cycles on the slope of the embankment cause significant damage to the crushed-rocks embankment. For example, Figure 2(a) indicates a location on the slope of the Gongyu high-grade highway, where the crushed-rocks embankment has generated a large amount of debris. There are many types of crushed-rocks, including red sandstone, cyan sandstone, and granite. As shown in Figure 2(b), the pavement condition of the crushed-rocks embankment was used in the Gongyu high-grade highway.

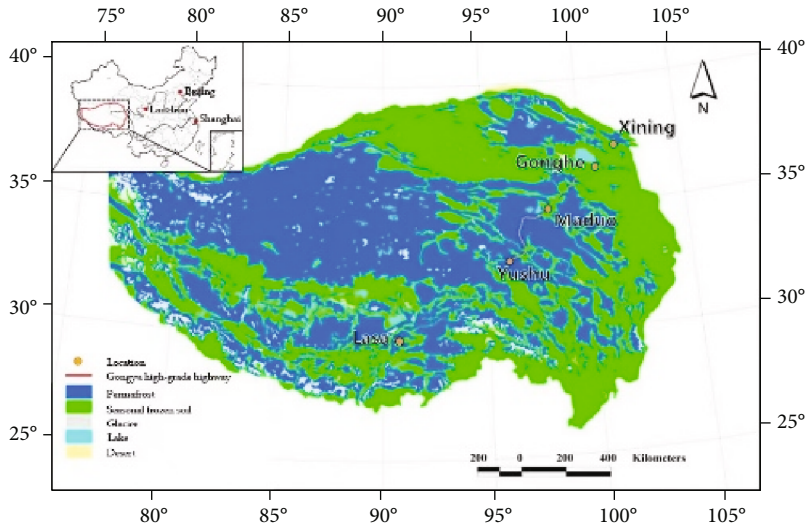


Figure 1: Distribution permafrost along the Gongyu high-grade highway.

(a) Weathering of slope crushed-rocks (b) Damage to pavement and pavement structures

Figure 2: Qinghai Province's Gongyu high-grade highway overview.

Much past work—both in China and globally—has focused on the damage done to rock from slope of subgrade or tunnel by freeze-thaw processes, mainly in the physical and mechanical properties. To this end and in 1985, Lemaitre first proposed the theory of damage mechanics based on the principle of irreversible mechanics. In the special environment presented by alpine regions, the frequent alternation of cold and hot leads to complex damage and mechanical properties of the crushed-rocks under freeze-thaw cycles. Feng et al. [7] studied the stress-strain relationship of rocks under different freeze-thaw cycles. They proposed a new piecewise constitutive model based on the characteristics of stress-strain curves after compaction and compaction. Chun et al. [8] used a nuclear magnetic resonance nondestructive testing technique to detect damage in crushed-rocks. Similarly, Javad et al. [9] used indoor tests approaches to assess the physical and mechanical properties and damage behavior of sandstone under different freeze-thaw cycles. Similar to Javad et al.'s work, Jia et al. [10] subjected sandstone to 50 freeze-thaw cycles and measured the pore structure evolution using NMR method after each cycle. Their results indicated that changes of the sandstone pore structure were mainly caused by the expansion of nanopores and micropores as well as the generation of new nanopores. The resulting porosity showed an increasing-stabilizing-increasing trend with increasing freeze-thaw cycles; the permeability and surface roughness of the sandstone increased with increasing freeze-thaw cycles. Moreover, the pore size uniformity coefficient decreased linearly with increasing freeze-thaw cycles. Fu et al. [11] investigated different laminar angles (30°, 45°, 60°, and 75°) under different circumferential pressure conditions using triaxial compression tests. More specifically, the strength characteristics of freeze-thaw cores of carbonatite slate with different lamina angles of 30°, 45°, 60°, and 75° were investigated using triaxial compression tests. A statistical model of the triaxial compressive strength of each homogeneous crushed-rock based on the single discontinuity theory was then proposed. The test results showed that the triaxial compressive strength decreased with increasing number of freeze-thaw cycles. Moreover, strength continuously increased as the surrounding pressure increased. The validity and accuracy of the model were then verified by comparing with the test results. The model was able to better describe the effect of

Figure 3: On-site sandstone and granite.

the number of freeze-thaw cycles, surrounding pressure, and laminar surface orientation on the triaxial compressive strength of freeze-thaw isotropic crushed-rocks. Collectively, the freezing susceptibility of crushed-rocks was the result of the combined effect of pore network characteristics and the way water entered the pore network. Alice et al. [12] studied the effect of these parameters on freeze-thaw weathering of crushed-rocks and discussed the coupling effect of state parameters (dynamic elastic modulus) and transfer parameters (water permeability). Mu et al. [13] selected triaxial typical nodular crushed-rocks for multiple freeze-thaw tests. After the tests, the degradation characteristics of the joints were investigated by conducting direct shear tests on the jointed specimens of the crushed-rock material.

Based on these past studies, many scholars focus on the study of the damage performance of rocks. This paper takes the permafrost region as the background and the field rocks, including red sandstone, cyan sandstone, and granite as the experimental object to understand the strength of the crushed-rocks during the freezing and thawing process. And a damage model described in detail the damage variation of crushed-rocks under the coupling action of freeze-thaw, and load was then established and verified.

## 2. Experimental Materials and Procedures

*2.1. Preparation of Rock Samples.* Figure 3 shows the crushed-rocks taken from the site high-grade highway, indicating the red sandstone, cyan sandstone, and granite that were used as test stones for the study; according to previously published specifications [14, 15], the crushed-rocks were cut and polished into standard crushed-rock samples of 50 mm in diameter and 100 mm in height. Rock samples of the same type are taken from the same stone body. Further tests included assessing wave velocity, porosity, size, and appearance. Any crushed-rock samples that had large differences in these characteristics were removed. Ultimately, three samples of similar rock type were combined into one group. The crushed-rocks were divided into 9 groups in total, 27 total. Three samples from each group were subjected to freeze-thaw cycles in parallel experiments. The basic physical parameters of each crushed-rock type are shown in Table 1.

*2.2. Test Equipment.* The uniaxial compression tests were carried out by FRTX-1000 servo-controlled rock triaxial test system produced by GCTS (Geotechnical Consulting & Testing Systems) company, as shown in Figure 4. The test load rate is 0.05 mm/min.

*2.3. Test Procedure.* Briefly, the selected rock specimens were numbered and then put into the blast dryer at 110 °C for 36 h. After drying, specimens were put into the drying dish and cooled to room temperature and then put into a vacuum saturation device under 0.1 MPa pressure for 6 h. The specimens were then placed in the vacuum dish under atmospheric pressure for 4 h. After, specimens were removed, water was removed from their surfaces, and they were individually weighed. Based on this, rock specimen was then subjected to the freeze-thaw cycle test. After a certain number of freeze-thaw cycles, the specimen's wave speed was measured. The specimen was also subjected to a uniaxial compression test, and any changes in its appearance were noted.

*2.4. Freeze-Thaw Process.* According to the local climate temperature changes at the site, a temperature range of -25 °C to 15 °C in 2020 is what might be experienced on an annual basis. As shown in Figure 5(a), the annual temperatures from March to June and also from September to November were used for the high freeze-thaw cycle stage. This was done to facilitate temperature control and the frequency of freeze-thaw temperature. Given this, we used a temperature of 15 °C to -15 °C for 100 freeze-thaw cycles. The experimental specimens would be at a temperature of -15 °C temperature at 12 h and then thawed for 12 h, for an overall freeze-thaw cycle of 24 h. The temperature curve of this freeze-thaw process is shown in Figure 5(b). The total freeze-thaw cycles used were 0, 5, 10, 15, 20, 30, 50, 70, and 100, followed by uniaxial compression tests.

## 3. Experimental Results and Analysis

*3.1. Rock Physical Characteristics.* After the freeze-thaw cycle, red sandstone and granite both had lateral and circular cracks, while cyan sandstone did not have any cracks appear with any serious edge spalling. Many factors likely affected the freeze-thaw damage observed in the crushed-rock. The water content of red sandstone was approximately 2-10 times that of cyan sandstone and granite, respectively. Similarly, the porosity was approximately 3 and 30 times, respectively (Table 1). The density and strength of the red sandstone were also the lowest. As indicated by the water content, the higher the water content, the greater the porosity and the lower the density. As a result, there is a greater likelihood of damage, even with less severe freeze-thaw cycle

Table 1: Basic physical parameters of the rocks.

| Rock sample | Longitudinal wave speed $v/(m/s)$ | Dry density $\rho_d/(g/cm^3)$ | Saturated density $\rho_s/(g/cm^3)$ | Water content $\omega$/% | Porosity $n$/% |
|---|---|---|---|---|---|
| Red sandstone | 2193 | 2.01 | 2.20 | 1.47 | 20.14 |
| Cyan sandstone | 2604 | 2.26 | 2.33 | 0.78 | 7.28 |
| Granite | 4464 | 2.59 | 2.60 | 0.13 | 0.62 |

Figure 4: Test equipment.

conditions. Given this, porosity and water content are the main factors affecting the damage observed in the crushed-rock. More specifically, the process of low-temperature freezing results in water turning to ice and increasing its ice volume. In a specimen with a larger pore size, specimen expansion occurs and produces greater pressure on the pore wall. As a result, the crushed-rock fractures continue to expand. When the specimen transitions from the frozen state to the melting state, the ice melts into water, and a negative pressure area will be formed in the pore. When the crushed-rock is refrozen, the water is frozen again. Under the condition of cyclic freezing and thawing, the original pores and crushed-rock defects are increased and destroyed, resulting in cracks. Given this, it is understandable why the freeze-thaw cycles used in this paper had a greater effect on red sandstone and a lesser one on granite. Additionally, there is the difference of crack production and its relationship to the distribution of pore space and subsequent development and distribution of joint fractures and stratification of the crushed-rock. Given this, the larger the pore space, the more easily water enters. This ultimately intensifies the development of cracks. With increasing number of freeze-thaw cycles, the red sandstone subjected to 5 freeze-thaw cycles had 2 cracks appear, while the surface of free particles had increased. Cracks continued to develop until after 50 cycles, at which point the specimens were fluffed outward and particles were continuously flaking. Similarly, the apparent changes of the saturated cyan sandstone appeared with increasing of freeze-thaw cycles. Compared to the red sandstone, the cyan sandstone had no cracks until the end of the cycle, at which point the edges were increasingly flaking. The granite cracks also appeared earlier, with the earliest also appearing after 5 freeze-thaw cycles and as 60° oblique cracks. With increasing number of freeze-thaw cycles, curved type cracks also appeared but only on the surface. The cracks continued to grow before 100 cycles was reached, with new cracks also appearing elsewhere.

*3.2. Wave Velocity Variation Curve.* The trend of the longitudinal wave velocity of the three crushed-rocks after 100 freeze-thaw cycles is shown in Figure 6. As indicated, the following characteristics are shown: Granite had the largest longitudinal wave velocity, with red sandstone having the smallest. The longitudinal wave velocity of the three crushed-rocks decreased with increasing number of freeze-thaw cycles. Of these, the longitudinal wave velocity of the red sandstone decreased the fastest and at the greatest magnitude. Red sandstone continued to decline even after 50 cycles. The main reason for its decline was that the freeze-thaw cycles made the internal mineral particles of the crushed-rock move unevenly up and down; this resulted in the development of fissures so that the wave velocity slowed down. Since the porosities of both cyan sandstone and granite were the smallest, these specimens were denser and the wave velocity did not change much. As a result, the freeze-thaw cycles had less effect on both cyan sandstone and granite.

*3.3. Stress-Strain Relationship.* Figure 7 shows the typical stress-strain curves of the three types of crushed-rocks. As indicated, the crushed-rock strength change curve can be divided into six stages: (1) Compaction stage (0-a), the pores and microfractures can withstand a very little force, so the application of even a small force can make them a close contact. This stage does not result in damage, but lets them become more compact. (2) In the elastic stage (a-b), with an increasing load, strain with stress can be considered according to the concept of statistical damage model. In sum, slight mechanical damage occurs at this stage. (3) In the elastic-plastic stage (b-c), damage has occurred inside the crushed-rock and microfractures also continue to develop. Crushed-rock particles slip, microfractures extend in the direction of the main direction of pressure, irreversible deformation of the crushed-rock occurs, the amount of deformation increases nonlinearly with increasing stress, and the test curve slows down. Overall, the crushed-rock integrity decreases. (4) In the yielding stage (c-d), the main mechanical damage inside the specimen is formed and continuously assembled, and the elastic modulus of the crushed-rock is continuously reduced. (5) After the residual stage (d-e) reaches the maximum strength, the strength of the rock decreases continuously, and the microcracks develop rapidly around, forming a main crack. The internal

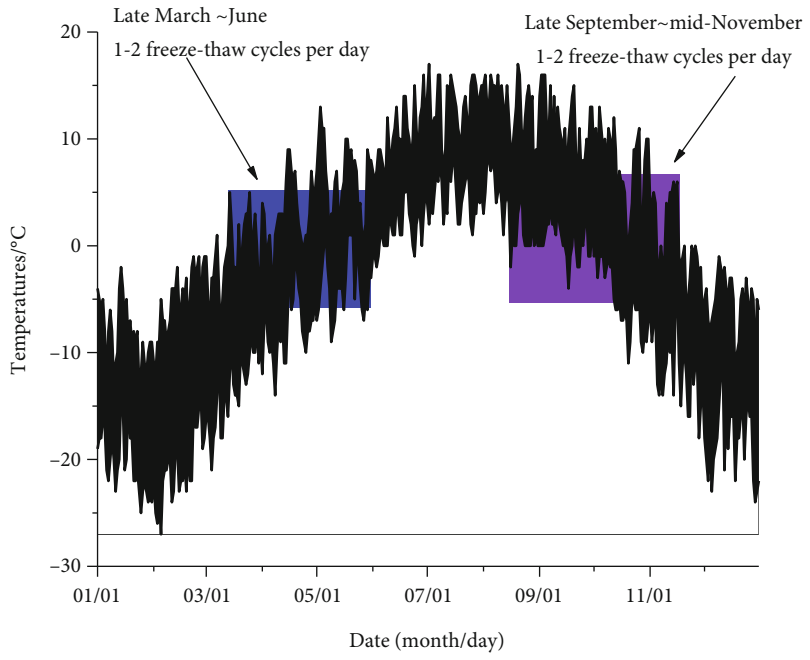


(a) Temperature trend in 2020

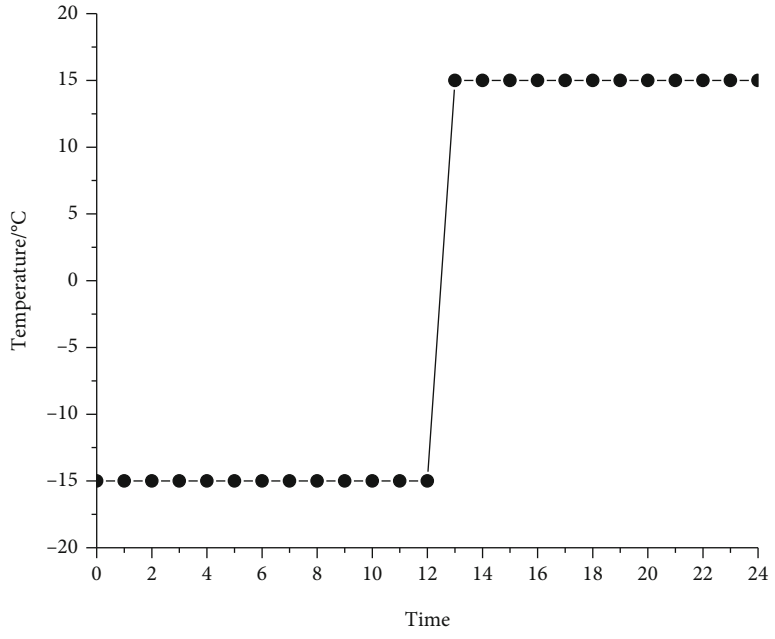


(b) Freeze-thaw cycle temperature change

Figure 5: Temperature variation.

structure of the rock is destroyed, and the strength decreases rapidly with the increase of deformation. The stress-strain curve is concave and the slope is negative. The main phenomenon is that the force decreases quickly and the rock increase the rock deformation. (6) In the damage stage (after the e point), the main fracture between the crushed-rock bonding force is zero, reaching a certain strength and resulting in the overall damage. Damage occurs quickly, rock the volume of damage rapidly increases, and the elastic modulus decreases. Red sandstone is in the elastic-plastic stage for a longer until the destruction stage, indicating that red sandstone plasticity is stronger. Cyan sandstone in the c stage after destruction is short and of quick duration. Cyan sandstone overall brittles stronger. Due to its higher strength, granite reached its peak and could withstand a larger amount stress and last for a longer period of time. After reaching the ultimate strength, granite was rapidly destroyed and went instantly to zero. As indicated from Figure 7(d), increasing freeze-thaw cycles resulted in three notable characteristics in the stress-strain curve of red sandstone: (1) The stress-strain curve became longer during the compaction stage, with obvious nonlinearity. (2) The stress-strain curve

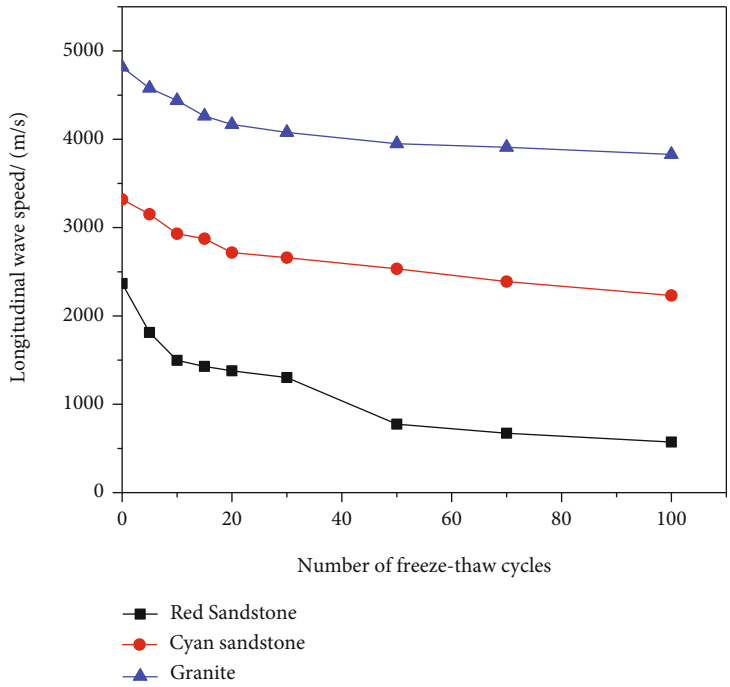


Figure 6: Wave speed variation curve.

tended to be arc-shaped when the red sandstone was close to destruction, with a decreasing slope of the curve. (3) The uniaxial compressive strength and elastic modulus kept decreasing, and the stress-strain curve was closer to an arc shape. The corresponding axial strain kept increasing, indicating that the plasticity also kept increasing. Taken together, these results indicate that the pores and microcracks inside the saturated red sandstone increased during the freeze-thaw process. Moreover, the internal damage kept increasing, leading to enhanced plasticity. Comparatively, the granite—which was relatively dense—had almost no effect on the internal damage as the water only existed on the surface under vacuum pressure.

*3.4. Variation Pattern of Peak Strength and Elastic Modulus of Crushed-Rocks.* To better study the effect of freeze-thaw cycles on the compressive strength of the three crushed-rocks, the change law of uniaxial compressive strength and elastic modulus of the crushed-rock samples with increasing number of freeze-thaw cycles was plotted according to the test data (Figure 8).

Fitting the points in Figure 8 yielded the following results for the fit between the number of freeze-thaw cycles and the uniaxial compressive strength and modulus of elasticity:

$$\text{Red Sandstone} \quad \sigma_b = 3.98 + 13.17e^{\left(-\frac{n-1.89}{51.34}\right)}, \tag{1}$$

$$\text{Cyan Sandstone} \quad \sigma_b = 19.81 + 27.52e^{\left(-\frac{n-137.77}{294.6}\right)}, \tag{2}$$

$$\text{Granite} \quad \sigma_b = 136.05 + 36.81e^{-\frac{n}{30.76}}, \tag{3}$$

$$\text{Red Sandstone} \quad E_1 = 1.05 + \frac{6.87}{1 + e^{n-5.65/24.31}}, \tag{4}$$

$$\text{Cyan Sandstone} \quad E_2 = 15.6 - 0.07n + 6.48n^2 - 3.52n^3, \tag{5}$$

$$\text{Granite} \quad E_3 = 65.22 - 0.2n + 0.004n^2 - 2.73n^3. \tag{6}$$

From the equation fitting results, the uniaxial compressive strength decreased exponentially with increasing number of freeze-thaw cycles. Freeze-thaw cycles had a greater impact on the uniaxial compressive strength of crushed-rocks. When crushed-rocks are washed by rain, free water enters the crushed-rock interior along the pore space. This free water is converted into ice at low temperatures, causing the crushed-rock volume to expand and produce a frost swelling force that accelerates the generation and development of cracks. Continuous circulation reduces the cementation of mineral particles, resulting in an overall decrease of crushed-rock strength.

The freeze-thaw coefficient is an important parameter in crushed-rock mechanics and describes the ability of crushed-rocks to resist weathering. The freeze-thaw coefficients of three types of crushed-rocks can be derived from the following equations:

$$K_f = \frac{\overline{R_f}}{\overline{R_s}}, \tag{7}$$

where $K_f$ is the freeze-thaw coefficient, $\overline{R_f}$ is the average saturated uniaxial compressive strength after the freeze-thaw test (MPa), and $\overline{R_s}$ is the average saturated uniaxial compressive strength before the freeze-thaw test (MPa).

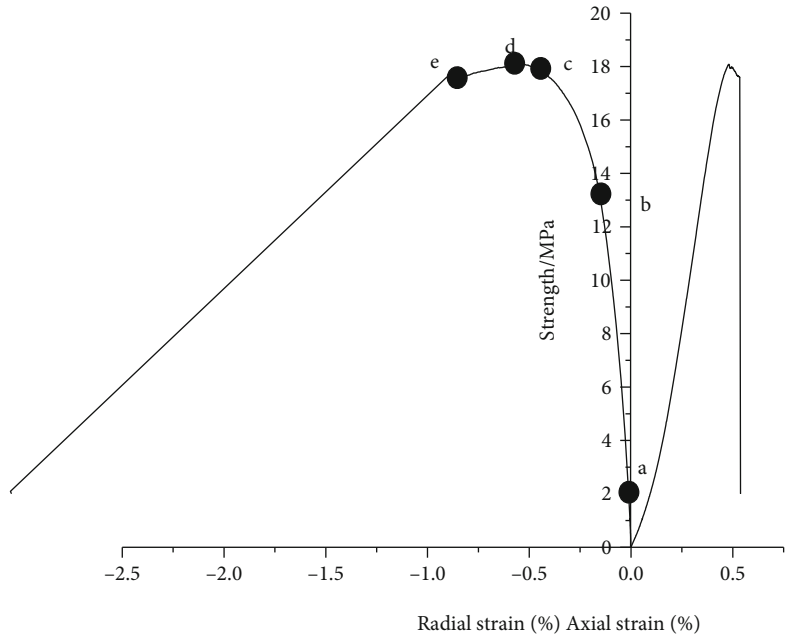


(a) Red sandstone

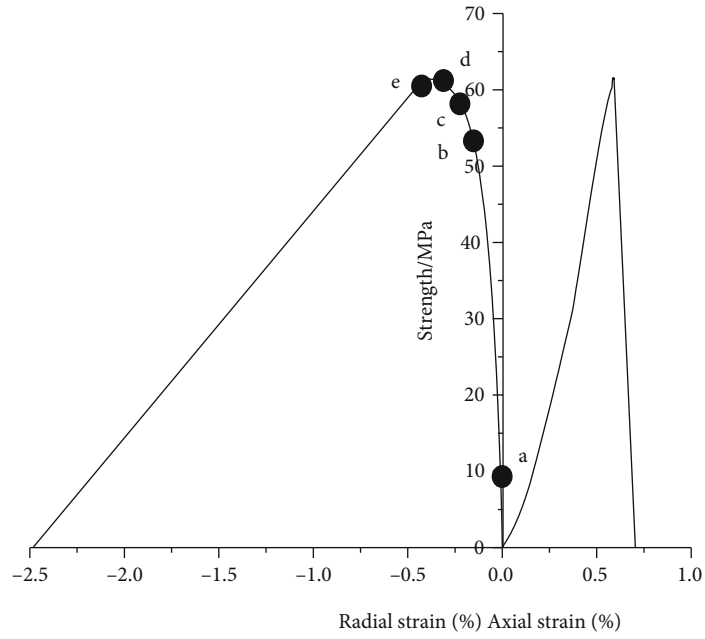


(b) Cyan sandstone

Figure 7: Continued.

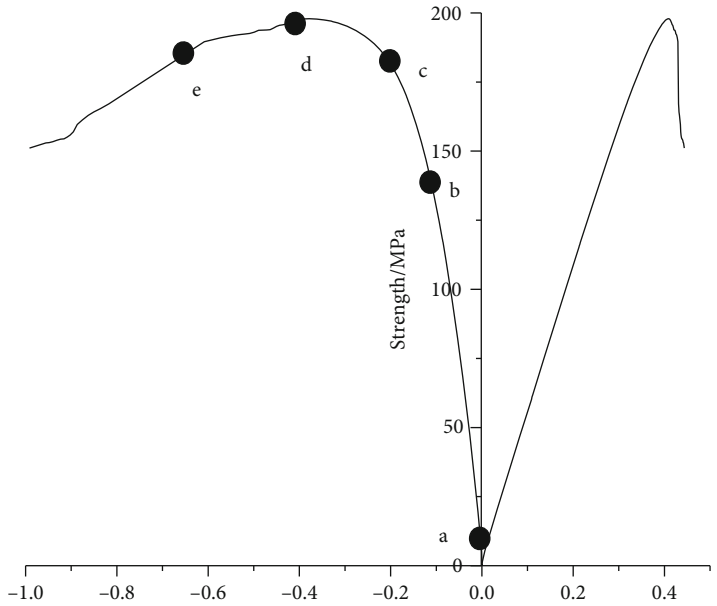


(c) Granite

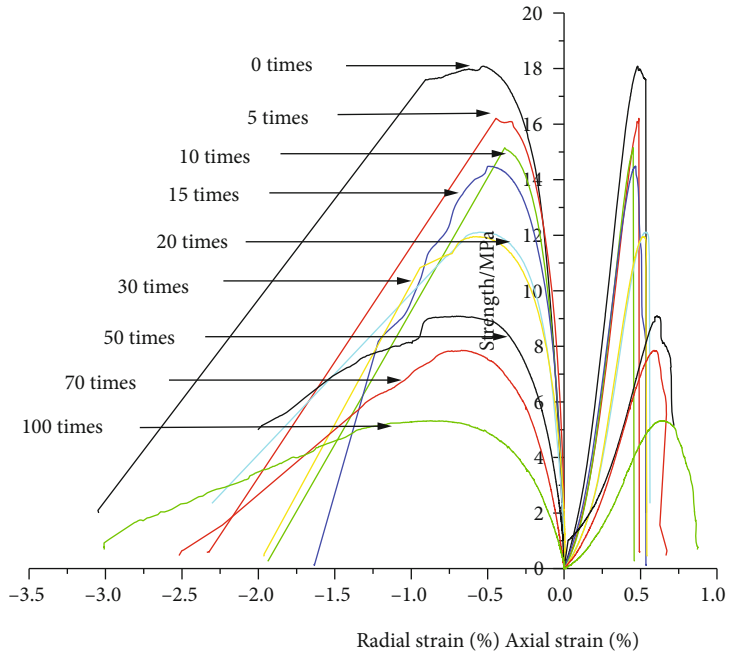


(d) Red sandstone with different freeze-thaw cycles

Figure 7: Stress-strain relationship of different rock.

From Equation (7), the freeze-thaw coefficient of the three crushed-rocks can be calculated, as shown in Table 2.

As shown in the table, the number of freeze-thaw cycles had a greater effect on red sandstone, whose freeze-thaw coefficient decreased significantly. The number of freeze-thaw cycles had little effect on both cyan sandstone, whose freeze-thaw coefficient changed slowly, and granite, whose freeze-thaw coefficient tended to remain constant after 50 freeze-thaw cycles.

*3.5. Study of Microscopic Damage in Crushed-Rocks under Freeze-Thaw Conditions.* To study the effect of freeze-thaw cycles on the microscopic morphology of a road base using crushed-rocks, we conducted electron microscopy scanning experiments on the specimens after they had been subjected freeze-thaw cycles. Given the above findings, the uniaxial compressive strength of the specimens was greatly changed after 5 and 20 freeze-thaw cycles. As a result, a microscopic experimental study after the number of freeze-thaw cycles

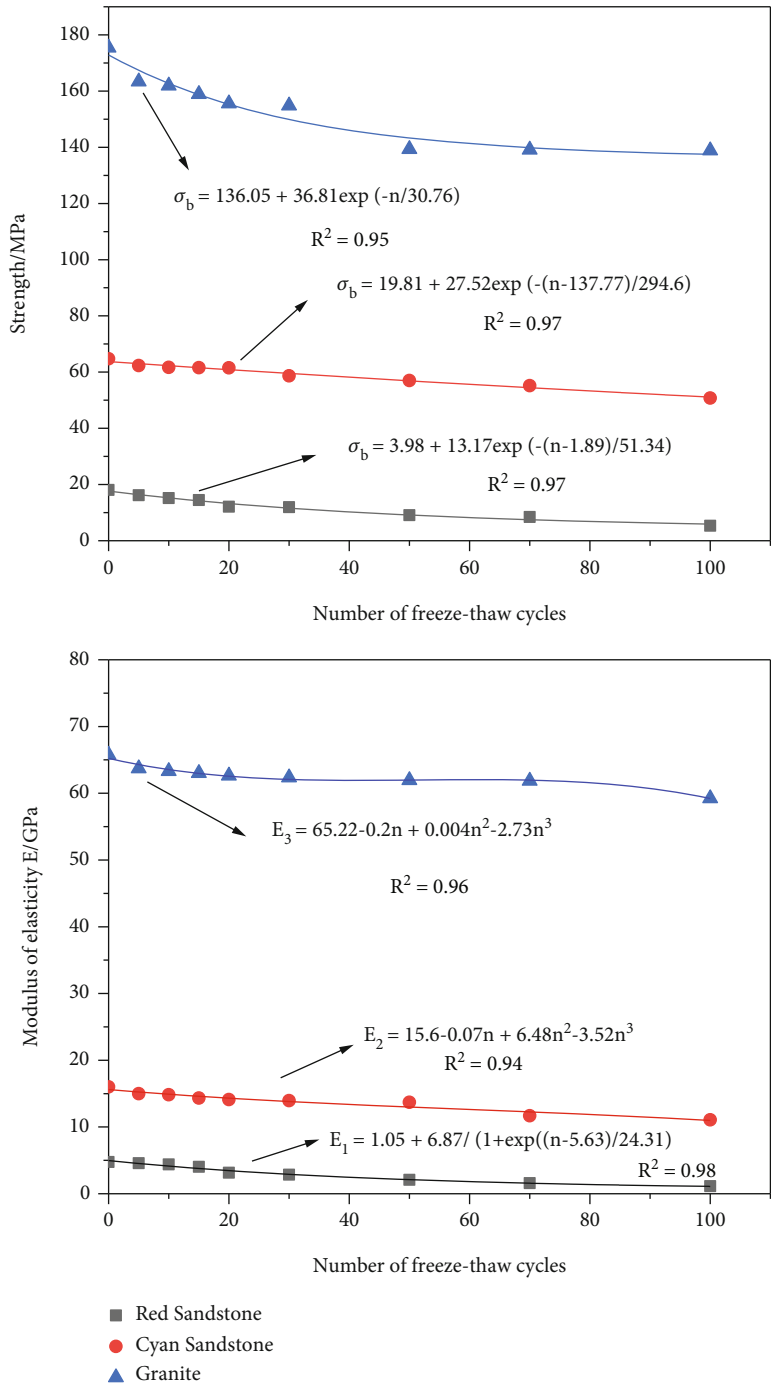


Figure 8: Curve of the effect of freeze-thaw cycles on the three types of crushed-rocks.

Table 2: Relationship between freeze-thaw coefficients and the number of freeze-thaw cycles for three types of crushed-rocks.

| Category | Freeze-thaw coefficient $K_f$ | | | | | | | | |
|---|---|---|---|---|---|---|---|---|---|
| | 0 | 5 | 10 | 15 | 20 | 30 | 50 | 70 | 100 |
| Red sandstone | 1.0 | 0.89 | 0.84 | 0.80 | 0.67 | 0.66 | 0.50 | 0.47 | 0.29 |
| Cyan sandstone | 1.0 | 0.96 | 0.95 | 0.95 | 0.95 | 0.90 | 0.88 | 0.85 | 0.78 |
| Granite | 1.0 | 0.93 | 0.92 | 0.90 | 0.89 | 0.88 | 0.79 | 0.79 | 0.79 |

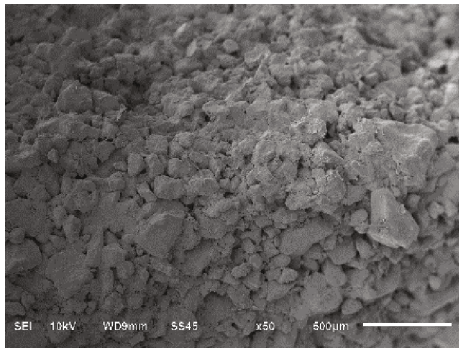

(a) 5 freeze-thaw cycle

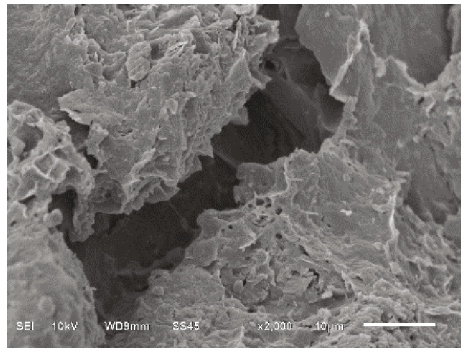

(b) 5 freeze-thaw cycle

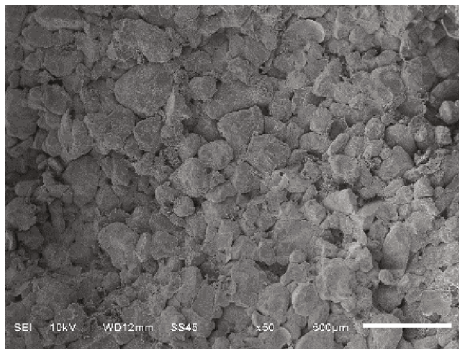

(c) 20 freeze-thaw cycle

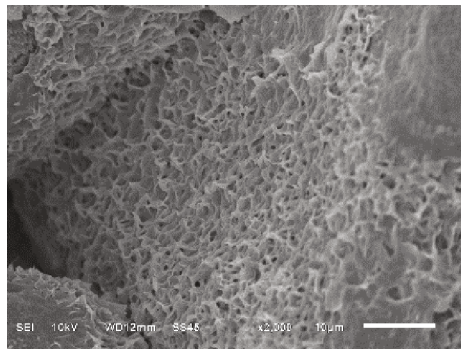

(d) 20 freeze-thaw cycle

Figure 9: SEM images of red sandstone at different freeze-thaw times at 50 and 2000.

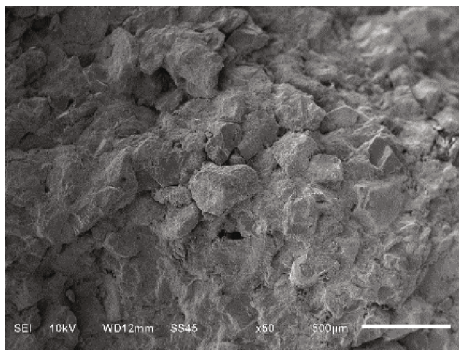

(a) 5 freeze-thaw cycle

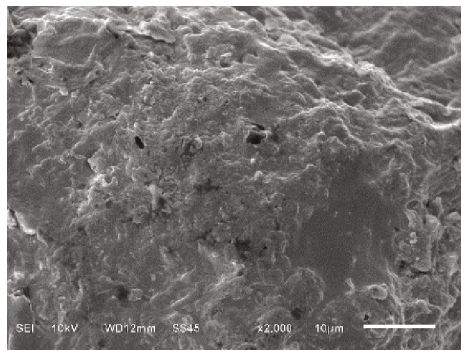

(b) 5 freeze-thaw cycle

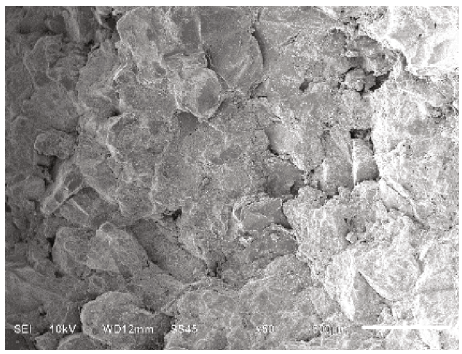

(c) 20 freeze-thaw cycle

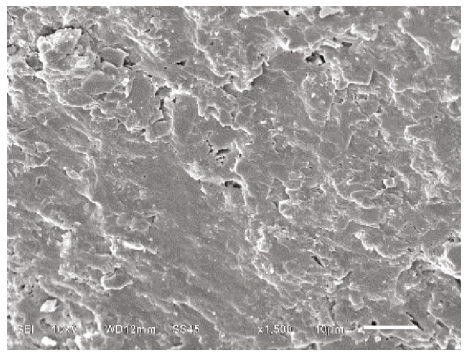

(d) 20 freeze-thaw cycle

Figure 10: SEM images of cyan sandstone at 50 and 2000 times under different number of freeze-thaw cycles.

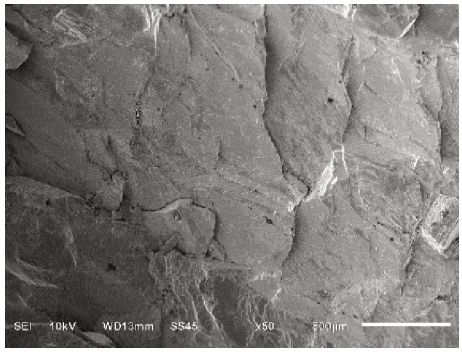

(a) 5 freeze-thaw cycle

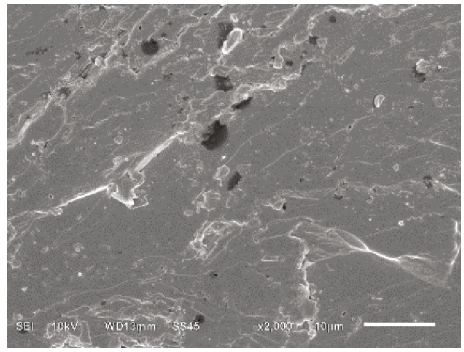

(b) 5 freeze-thaw cycle

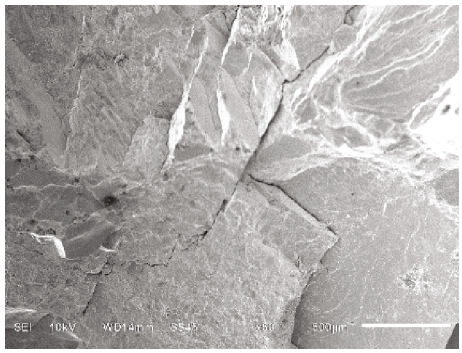

(c) 20 freeze-thaw cycles

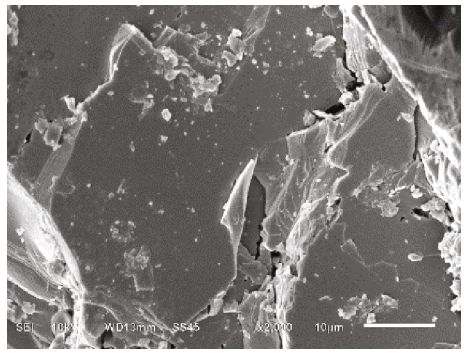

(d) 20 freeze-thaw cycles

Figure 11: SEM images of granite at 50 and 2000 times under different number of freeze-thaw cycles.

was conducted Figures 9 –11. As shown and after 5 freeze-thaw cycles, the red sandstone had lower microporosity and less pores, and there was a cement link between the mineral particles. The link was denser, and there were a few pores on the surface of the particles after magnification. With increasing freeze-thaw cycles and after 20 cycles, the particles were looser, and the pores on the surface of the particles had increased. Moreover, the honeycomb structure was connected. The main reason for this was that during the freezing and thawing process, the mineral cement of the crushed-rock particles was dissolved and disintegrated. The free water phase change inside the crushed-rock then produced freezing and swelling forces, allowing for the micropores and micro fissures of the crushed-rock to form, expand, and connect by the freezing and swelling forces. As a result, the cementing ability between the mineral particles was weakened and the micropores on the surface of the particles increased in number. When compared with red sandstone, the link between the particles was denser, which was also one of the reasons why cyan sandstone, was stronger than red sandstone. The microporosity of cyan sandstone was not as obvious as that of red sandstone. The pores of granite were also not obvious, the joints were more obvious, the microcracks had increased, the surface was rough, and the loose particles had increased. This was mainly because the weak parts of the mineral particles had started to disintegrate under the effects of freezing and hydration. This resulted in the formation of some loose particles that were attached to the surface. The growth of cracks also increased under the same freezing and swelling forces.

## 4. Damage Model for Freeze-Thaw and Load of Crushed-Rocks

*4.1. Constitutive Model for Freeze-Thaw and Load Damage.* The combined effects of long-term outflow of crushed-rocks onto the slope and road area along with erosion caused by rainwater, temperature changes, and load will cause microstructural changes and deterioration of the force properties of the crushed-rock. To a certain extent, these microstructural changes will lead to easier weathering and degraded mechanical properties of the crushed-rock. To this end, crushed-rock damage is a continuous process of accumulation. According to the definition of macroscopic phenomenological damage mechanics, it is considered that the response of macroscopic physical properties can reflect the degree of internal deterioration of the materials. Benchmarks for measuring damage such as elastic modulus, yield stress, and ultrasonic velocity can then be selected. Therefore, the elastic modulus not only reflects the change law of crushed-rock mechanics, but is also useful as the damage variable itself. Given this, the damage variable caused by crushed-rock freezing and thawing can be defined as

$$D_n = 1 - \frac{E_n}{E_0}, \tag{8}$$

where $E_0$ is the initial modulus of elasticity of the crushed-rock before freeze-thaw and $E_n$ is the modulus of elasticity of the crushed-rock after the nth freeze-thaw cycle.

According to the strain equivalence principle proposed by Lemaitre, the strain caused by full stress acting on the damaged material is equivalent to the strain caused by the effective stress acting on the undamaged material. By replacing the full stress with the effective stress, the constitutive relationship of the damaged material can be derived from the undamaged material. Promote the principle of post-strain equivalence; that is, if any two of the damage states are taken, the strain caused by the effective stress acting on the second damage state of the material in the first damage state is equivalent to the strain caused by the effective stress acting on the first damage state of the material in the second damage state. Most of the crushed-rocks in nature occur with initial damage. The damage caused by freezing and thawing is the first damage state, and the damage caused by the load after freezing and thawing is the second damage state. The principal equation of the crushed-rock in the two damage states is obtained as

$$\sigma_{\mathrm{n}} = E_0(1 - D_{\mathrm{n}})\varepsilon_{\mathrm{n}} \quad \sigma = E_{\mathrm{n}}(1 - D)\varepsilon, \tag{9}$$

where $E_{\mathrm{n}}$ is the modulus of elasticity of the crushed-rock after freezing and thawing and $D$ is the damage variable under load.

Now substitute Equation (8) into Equation (9) to obtain the crushed-rock freeze-thaw stress-strain relationship expressed by the crushed-rock freeze-thaw damage variable as

$$\sigma = E_0\left(1 - D_{\mathrm{g}}\right)\varepsilon. \tag{10}$$

One of

$$D_{\mathrm{m}} = D + D_{\mathrm{n}} - DD_{\mathrm{n}}, \tag{11}$$

where $\sigma$ is the stress component, $\varepsilon$ is the strain component, $D_{\mathrm{m}}$ is the total damage of the crushed-rock by freeze-thaw and load, $D$ is the damage caused by the crushed-rock by loading, and $DD_{\mathrm{n}}$ is the coupling term. As indicated from Equation (11), the joint action of freeze-thaw and load increases the damage of the crushed-rock. However, the damage caused by freeze-thaw and the damage caused by loading are not simply superimposable, and the coupling term shows that the coupling of the two phases deteriorates the total damage. The freeze-thaw cycle causes damage to the internal microstructure, and the close fitting between the microporous closed particles inside the crushed-rock after loading. The microscopic defects are improved to reduce the damage caused by freeze-thawing.

*4.2. Crushed-Rock Damage Evolution Equation.* Crushed-rock material damage is a cumulative damage process, which is physically reflected as the process of accumulated microstructural changes. Mechanically, it is the accumulation process of macroscopic defect generation and expansion. Ultimately, this process will lead to the deterioration of the material. When considering the damage of crushed-rock material during loading as a continuous process, the distribution of fine defects inside the crushed-rock has certain randomness. After the crushed-rock is subjected to external action, its internal microdefects continuously change. Penetration occurs in some areas, leading to the formation of macroscopic cracks and resulting in crushed-rock damage.

The crushed-rock can be divided into an infinite number of microelements. Assuming that the strength of microelements obeys the Weibull distribution and its damage probability density function can be expressed by the material strain $\varepsilon$:

$$P(\varepsilon) = \frac{\mathrm{k}}{\lambda}\left(\frac{\varepsilon}{\lambda}\right)^{\mathrm{k}-1} \mathrm{e}^{-\left(\frac{\varepsilon}{\lambda}\right)^{\mathrm{k}}}, \tag{12}$$

where $P(\varepsilon)$ is the distribution function of crushed-rock microelement strength and both $\lambda$ and k values are distribution parameters that can be obtained from the test data.

Assuming that the statistical damage variable $D$ under a certain load is the ratio of the number n of damaged microelements to the total number $N$, namely,

$$D = \frac{\mathrm{n}}{N}. \tag{13}$$

Suppose that the number of equivalent microelements that produce damage in any interval $[\varepsilon, \varepsilon + d\varepsilon]$ is $NP(\varepsilon)\mathrm{d}\varepsilon$ and the number of equivalent microelements that have been damaged when loaded to a certain level $\varepsilon$ is

$$n = \int_0^{\varepsilon} NP(\varepsilon)\mathrm{d}\varepsilon = N\left[1 - \mathrm{e}^{-\left(\frac{\varepsilon}{\varepsilon_0}\right)^{\mathrm{k}}}\right], \tag{14}$$

where $k = 1/\ln\left(E_0\varepsilon_0/\sigma_0\right)$ is the material parameter characterizing the damage evolution of the material and $\varepsilon_0$ is the strain value corresponding to the peak $\sigma_0$.

Bringing Equation (14) into Equation (13), the statistical damage evolution equation for crushed-rocks subjected to load is obtained as

$$D = 1 - \mathrm{e}^{-\left(\frac{\varepsilon}{\varepsilon_0}\right)^{\mathrm{k}}}. \tag{15}$$

From Equations (8), (11), and (15), the total damage evolution equation with the number of freeze-thaw cycles and strain as the damage evolution control variables can be obtained as

$$D_{\mathrm{m}} = 1 - \frac{E_{\mathrm{n}}}{E_0}\mathrm{e}^{-\left(\frac{\varepsilon}{\varepsilon_0}\right)^{\mathrm{k}}}. \tag{16}$$

From the above equation and when only freeze-thaw damage is considered, the load strain $\varepsilon = 0$, at the time $D_m = D_n$; when only load damage is considered, $E_0 = E_n$, at the time $D_m = D$.

Considering $D_m$ as a function of $x(n, \varepsilon)$, when the number of freeze-thaw and strain changes, the equation of the total damage evolution rate of the crushed-rock can be obtained from Equation (16) and Equation (8) as

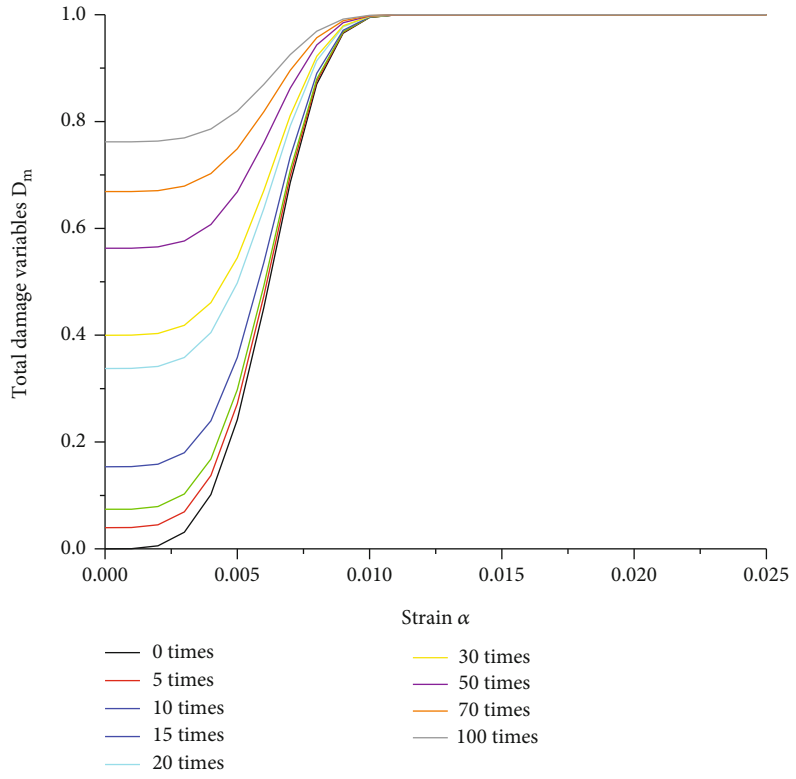


(a) Red sandstone

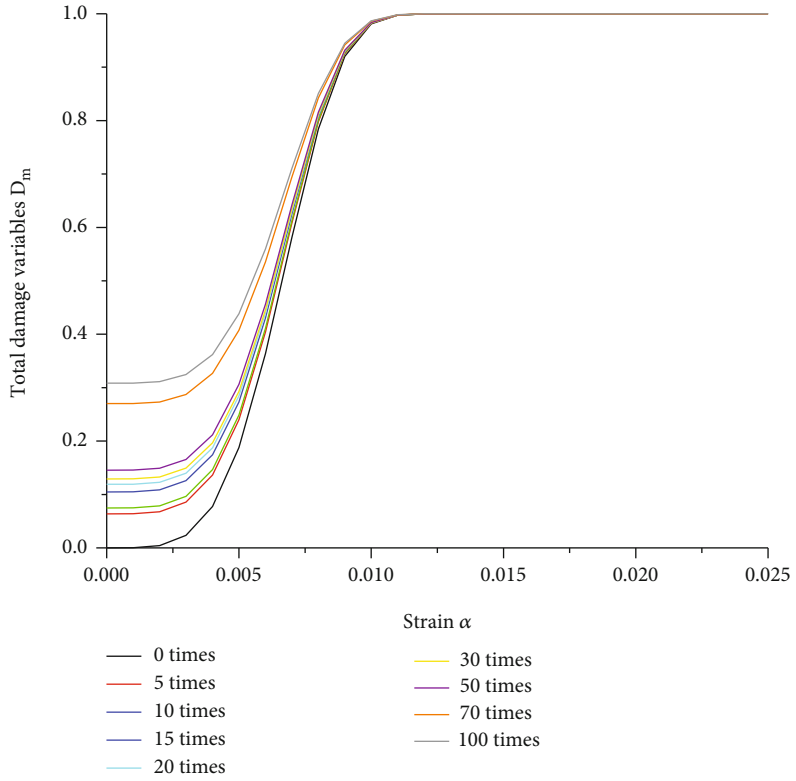


(b) Cyan sandstone

Figure 12: Continued.

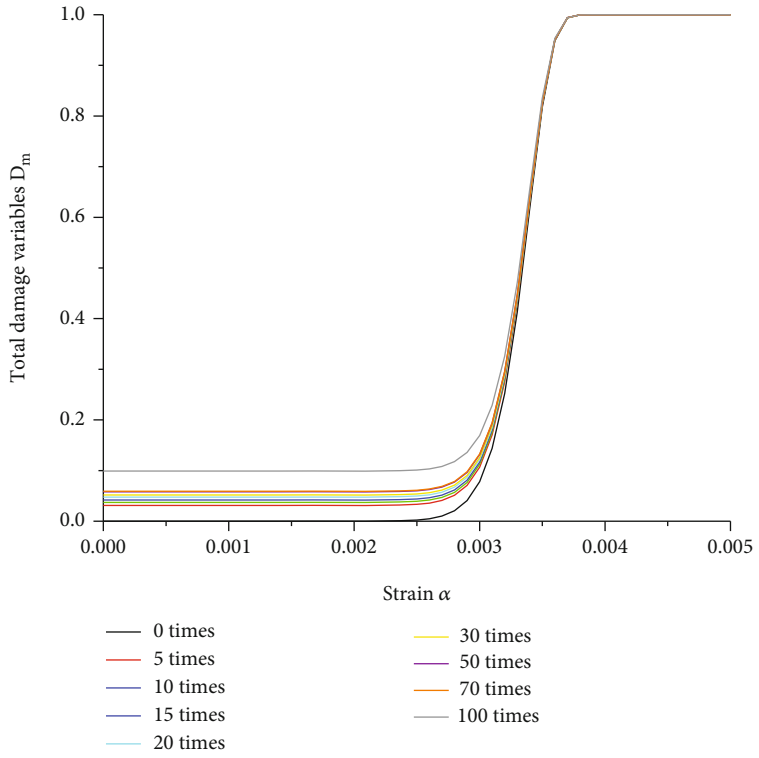


(c) Granite

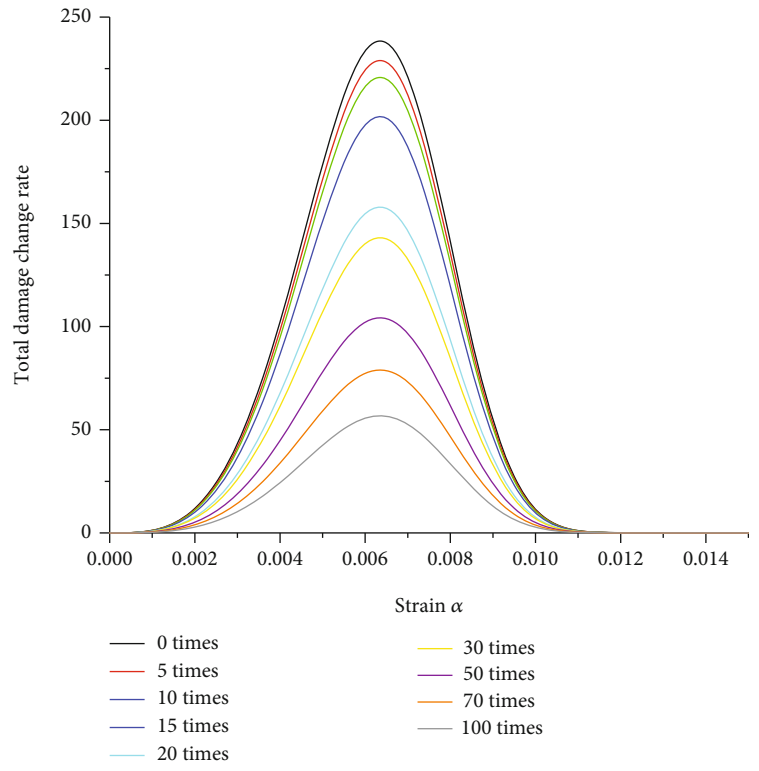


(d) Red sandstone

Figure 12: Continued.

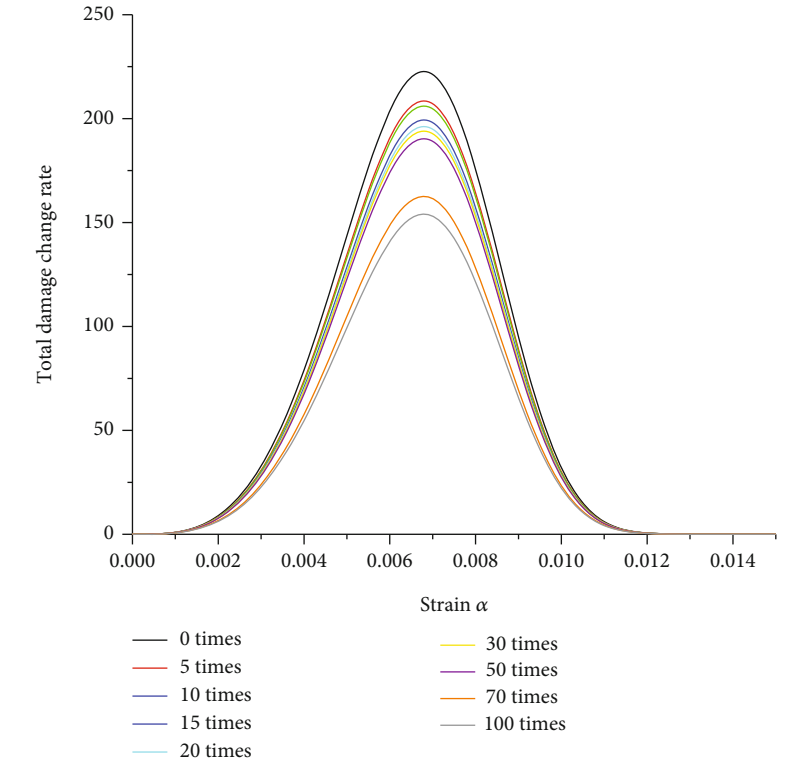


(e) Cyan sandstone

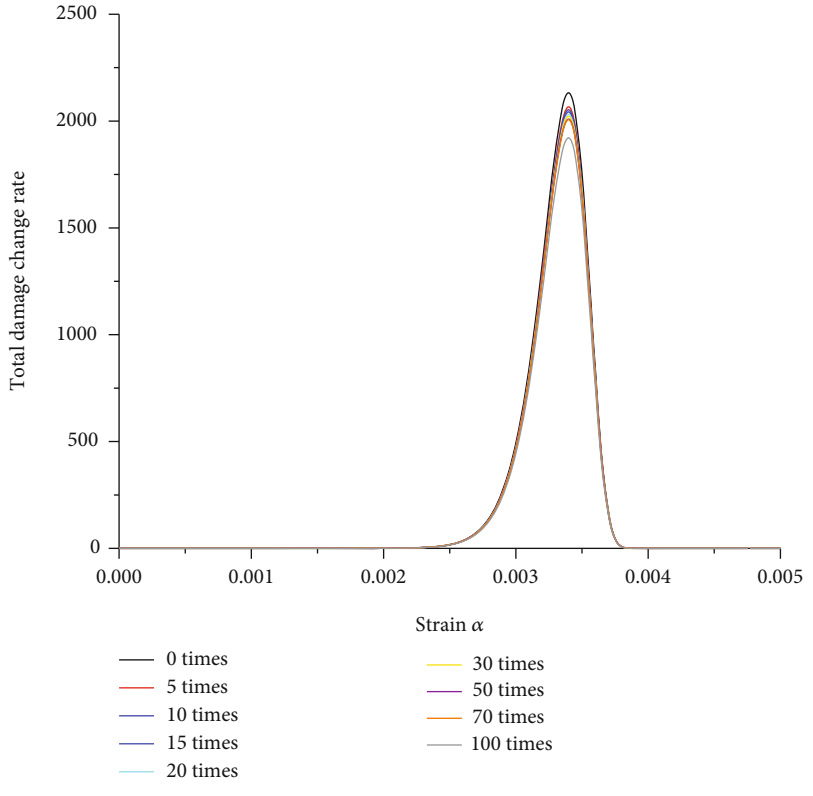


(f) Granite

Figure 12: Variation curves of freeze-thaw damage model and damage rate of three types of crushed-rocks.

$$\frac{\partial D_{\mathrm{m}}}{\partial \mathrm{x}} = (1 - D_{\mathrm{n}})\frac{\partial D}{\partial \varepsilon} + (1 - D)\frac{\partial D_{\mathrm{n}}}{\partial \mathrm{n}} = \frac{E_{\mathrm{n}}}{E_0}\frac{\varepsilon^{\mathrm{k}-1}}{\varepsilon_0^{\mathrm{k}}}\mathrm{e}^{-\left(\frac{\varepsilon}{\varepsilon_0}\right)^{\mathrm{k}}}. \quad (17)$$

The total damage of crushed-rock freeze-thaw and load varies along the two evolutionary paths of freeze-thaw and strain, reflecting the characteristics of coupling and mutual influence of the number of freeze-thaw cycles and strain on material damage expansion. This can reveal the mechanical behavior of crushed-rock material damage and damage expansion law in a more realistic way.

Bringing Equations (16) into Equation (10) to obtain the crushed-rock freeze-thaw load ground damage constitutive relationship as

$$\sigma = E_{\mathrm{n}}\mathrm{e}^{\left[-\left(\frac{\varepsilon}{\varepsilon_0}\right)^{\mathrm{k}}\right]}\varepsilon. \quad (18)$$

## 5. Model Validation

The following Figures 12(a) to 12(c) show the evolution curves of the freeze-thaw and load damage model for three types of crushed-rocks using the experimental data presented in this paper, obtained from Equation (16) and the test parameters of freeze-thaw mechanical properties. As shown, the following are observed: (1) As a whole, the degree of freeze-thaw damage of crushed-rock increased with increasing freeze-thaw cycles. Compared with zero freeze-thaw cycles, the degree of freeze-thaw damage varied greatly. (2) When the degree of damage was the same, the strain of crushed-rock decreased with increasing freeze-thaw cycles. (3) When the same strain occurred, with increasing the number of freeze-thaw cycles increased the damage. (4) At the same number of freeze-thaw cycles, the freeze-thaw damage of red sandstone was worse than the other two crushed-rock types. After 100 cycles of freeze-thaw, the damage variable was close to 1 when the strain was approximately 0.7%, which was close to the actual stress-strain graph. At this time point, the red sandstone was close to disintegration owing to the influence of the freeze-thaw cycles. Given this, its freeze-thaw durability was very poor. (5) The strain value of granite damage variable tended to 1 under different freeze-thaw cycles is almost close, which indicated that the number of freeze-thaw cycles had a little effect on its ultimate strength. This meant that the load damage caused the granite to be damaged.

The expressions for the three crushed-rock freeze-thaw damage variables $D(\mathrm{n})$ fitted to the freeze-thaw cycle test data as a function of the number of freeze-thaws n are

$$\text{Red Sandstone}: D(\mathrm{n}) = -0.026 + 0.016 - 8.202\mathrm{n}^2, \quad (19)$$

$$\text{Cyan Sandstone}: D(\mathrm{n}) = 0.033 + 0.003\mathrm{n} - 7.82\mathrm{n}^2, \quad (20)$$

$$\text{Granite}: D(\mathrm{n}) = 0.021 + 9.135\mathrm{n} - 2.127\mathrm{n}^2. \quad (21)$$

The total damage rate evolution curves of the three crushed-rocks calculated by Equations (8), (15), and (17) are shown in Figures 12(d) to 12(f). As indicated, the number of freeze-thaw cycles had the same damage evolution trend for the three crushed-rock types, with an increasing strain under the same number of freeze-thaw cycles. The damage rate of the three crushed-rocks showed a trend of first increasing in rate, reaching a peak rate of damage, and then decreasing. Each rock type had different values of its respective peak size. Under the same strain condition, the damage evolution rate of the red sandstone gradually decreased with increasing number of freeze-thaw cycles. This indicated its increasing plasticity. The area in Figures 12(d) to 12(f) reflects the magnitude of the total damage variable $D_{\mathrm{m}}$ value. The slope of the descending section after the peak of the granite is greater compared with the other two sandstones, indicating that the granite was more brittle.

## 6. Conclusions

Under the conditions of freeze-thaw cycles, the three kinds of crushed-rocks used in the embankment of crushed-rocks from the Gongyu high-grade highway in Qinghai Province were damaged to varying degrees. Among them, the red sandstone was the most seriously damaged by the freeze-thaw cycles and then cyan sandstone. Granite was only slightly damaged and only had some apparent cracks appear. The uniaxial compressive strength and elastic modulus of the rocks decrease with the increase of the number of freeze-thaw cycles. And the fitted curves and expressions better describe effects of freeze-thaw cycles on crushed-rocks.

As indicated from the representative SEM images of the three crushed-rocks, the red sandstone was composed of countless particles and had gaps between particles. With the increasing freeze-thaw cycles, a honeycomb structure was formed on the surface of the particles. The connection between the cyan sandstone particles was looser than prior to freeze-thaw, and more cracks appeared in the granite. The surface was rougher, and the loose particle number increased.

A mathematical model was used to characterize the complex relationship between freeze-thaw, load, and damage in crushed-rock. It can be seen from the model that the freeze-thaw cycle has a greater impact on red sandstone, followed by cyan sandstone and granite. The freeze-thaw and load damage model are similar to the test results, which indicates that the damage law of freeze-thaw cycles to rocks can be well described.

## Data Availability

The data used to support the findings of this study are included within the article.

## Conflicts of Interest

The authors declare that they have no conflicts of interest.

## Acknowledgments

This work was supported by the National Natural Science Foundation of China (Nos. 42161026 and 41801046), the

Natural Science Foundation of Qinghai Province (No.2021-ZJ-716), the China Railway Engineering Corporation Science and Technology Development Plan (2019-ZD-54), and the Major Project of Inner Mongolia Autonomous Region (ZDZX2018041).

## References

[1] Z. You-wu, Q. Guo-qing, G. Dong-xin, G. Qiu, and G. Chen, *Geocryology in China*, Science Press, Beijing, 2000.

[2] Q. Wang, J. Fang, X. Zhao, and K. Hu, "The influence of pavement type on the thermal stability of block-stone embankments in the warm permafrost region," *Transportation Geotechnics*, vol. 23, no. 11, article 100334, 2020.

[3] J. Latvala, H. Luomala, P. Kolisoja, and A. Nurmikolu, "Convective heat transfer in crushed rock aggregates: the effects of grain size distribution and moisture content," *Journal of Cold Regions Engineering*, vol. 34, no. 3, article 04020012, 2020.

[4] B. Sun, X. Xu, Y. Lai, D. Li, S. Wang, and J. Zhang, "Experimental researches of thermal diffusivity and conductivity in embankment ballast under periodically fluctuating temperature," *Cold Regions Science & Technology*, vol. 38, no. 2-3, pp. 219–227, 2004.

[5] Y. Dong, Y. Lai, J. Li, and Y. Yang, "Laboratory investigation on the cooling effect of crushed-rock interlayer embankment with ventilated ducts in permafrost regions," *Cold Regions Science and Technology*, vol. 61, no. 2-3, pp. 136–142, 2010.

[6] S. Zhizhong, M. Wei, and L. Dongqing, "In situ test on cooling effectiveness of air convection embankment with crushed rock slope protection in permafrost regions," *Journal of Cold Regions Engineering*, vol. 19, no. 2, pp. 38–51, 2005.

[7] F. Gao, X. Xiong, C. Xu, and K. Zhou, "Mechanical property deterioration characteristics and a new constitutive model for rocks subjected to freeze-thaw weathering process," *International Journal of Rock Mechanics and Mining Sciences*, vol. 140, article 104642, 2021.

[8] C. Yang, K. Zhou, X. Xiong, H. Deng, and Z. Pan, "Experimental investigation on rock mechanical properties and infrared radiation characteristics with freeze-thaw cycle treatment," *Cold Regions Science and Technology*, vol. 183, article 103232, 2021.

[9] J. Yahaghi, H. Liu, A. Chan, and D. Fukuda, "Experimental and numerical studies on failure behaviours of sandstones subject to freeze-thaw cycles," *Transportation Geotechnics*, vol. 31, article 100655, 2021.

[10] H. Jia, S. Ding, F. Zi, Y. Dong, and Y. Shen, "Evolution in sandstone pore structures with freeze-thaw cycling and interpretation of damage mechanisms in saturated porous rocks," *Catena*, vol. 195, article 104915, 2020.

[11] H. Fu, J. Zhang, Z. Huang, Y. Shi, and W. Chen, "A statistical model for predicting the triaxial compressive strength of transversely isotropic rocks subjected to freeze-thaw cycling," *Cold Regions Science and Technology*, vol. 145, pp. 237–248, 2018.

[12] A. Saad, S. Guédon, and F. Martineau, "Microstructural weathering of sedimentary rocks by freeze–thaw cycles: experimental study of state and transfer parameters," *Comptes Rendus Geoscience*, vol. 342, no. 3, pp. 197–203, 2010.

[13] J. Mu, X. Pei, R. Huang, N. Rengers, and X. Q. Zou, "Degradation characteristics of shear strength of joints in three rock types due to cyclic freezing and thawing," *Cold Regions Science and Technology*, vol. 138, pp. 91–97, 2017.

[14] Changjiang Academy of Science, *Changjiang Water Resources Commission, Code for rock tests in water and hydropower projects[S], SL/T264-2020*, Ministry of Water Resources of the People's Republic of China, Beijing, 2020.

[15] Zhongjiao Second Highway Survey and Design Institute, *Test methods of rock for highway engineering[S], JTG E41-2005*, Ministry of Communications of the People's Republic of China, Beijing, 2005.